RSC Advances

ROYAL SOCIETY OF CHEMISTRY

www.rsc.org/advances

Journal Name

RSCPublishing

COMMUNICATION

One-step Template-Directed Synthesis of Walnut-kernel- and Tremella-like Silica Spheres Composed of U-shaped Mesoporous Structures Based on pH-induced Colloid Aggregation

Cite this: DOI: 10.1039/x0xx00000x

Received 00th January 2012,
Accepted 00th January 2012

DOI: 10.1039/x0xx00000x

www.rsc.org/

Chunfeng Wang, [ab] Guowei Zhou,*, [a] Delan Xu, [a] Bin Sun, [a] Yan Zhang, [a] and Fengjiao Chen [a]

Synthesis of vesicular, walnut-kernel-, and tremella-like silica spheres (VSS, WKSS, and TSS) composed of hierarchical or U-shaped mesoporous structures were proposed by a pH-based approach. Spherical bodies with textural mesopores having sizes ranging from 30 to 40 nm were formed as a result of the diameter of U-shaped silica skeleton.

The development of silica-based nanomaterials with pore structures is currently an extensively researched topic, particularly with regard to their potential applications in areas such as adsorption, catalysis, separation, chromatography, sensor technology, and storage and controlled release,[1] because these nanomaterials offer advantages such as the possibility of surface modification and their robust mechanical properties and relatively inert chemical composition. Synthetic strategies of template fabrication have further enabled the production of silica-based nanomaterials with distinct shape features, with an increased interest in their applicability in variable structure systems. Silica-based nanoparticles with complex morphologies have been synthesized, for example, fibers,[2] rod-like powders,[3] sponge-like membranes,[4] monoliths,[5] polyhedral particles,[6] raspberry-like hollow spheres,[7] and vesicular nanospheres.[8] Recently, Li et al.[9] fabricated raspberry- and mulberry-like hierarchically structured silica particulate coatings via facile in situ layer-by-layer assembly with particles of two sizes, and they subsequently proposed the size ratio of these different-sized silica particles. To the best of our knowledge, no study has thus far attempted the surfactant-templating synthesis of walnut-kernel- and tremella-like silica spheres (WKSS and TSS) by a pH-induced colloid aggregation method. In this paper, therefore, we report the synthesis of vesicular silica spheres (VSS), WKSS, and TSS with a bimodal pore structure using a dual-templating system through a pH-based approach. In this system, tetraethyl orthosilicate (TEOS) is employed as the silica source, and the cationic surfactant cetyltrimethylammonium bromide (CTAB) and anionic surfactant sodium dodecyl sulfate (SDS) serve as a dual template for 4 to 5 nm mesopores. Furthermore, spherical bodies with textural mesopores having sizes from 30 nm to 40 nm are formed owing to voids between adjacent U-shaped silica particles. The influence of pH on the corresponding morphology and bimodal pore structure is also investigated.[15,16] Yan et al. used bolaamphipniles ($C_6PhC_6Na_2$) as template to observe its aggregation behavior at different pH values, and the results show that with the increase in pH values ($7.4<pH<11.5$), the aggregate morphology of $C_6PhC_6Na_2$ transformed from tubes to vesicles.[17]

Field emission scanning electron microscopy images of the representative samples synthesized with CTAB and SDS in different buffer solutions are shown in Figure 1. As shown in Figure 1a, most of the particles are intact spheres with diameters from 50 to 150 nm, and several particles are ruptured vesicular silicas, which could be attributed to the drying and calcination treatments of the sample; this figure shows these particles as being hollow spheres with relatively rough and thick shells. As seen in Figure 1b, rather surprisingly, the buffer solution with pH of 5.0 results in two different spherical structures, and it can be seen that minor amounts of TSS, except for ruptured hollow spheres, which is occasionally observed for less stable. To further probe the effect of pH of the buffer solution on the morphology, we fabricated samples using various buffer solutions with pH range of 7.0–10.0. As expected, significant amounts of WKSS and TSS were observed in Figure 1c and Figure 1d, whereas vesicular hollow spheres disappeared completely. In particular, it was clear that all samples (Figure 1e) exhibited better walnut-kernel-like morphology and uniformity. This was possibly an effect of the pH of the buffer solution on the morphology, i.e., on the shape of the micelles aggregation formed by a pH-based synthesis approach. Surprisingly, when pH was higher (i.e., 10.0), a small amount of irregular WKSS was formed (Figure 1f). With pH increased to an appropriate value, the silica spheres became more uniform; however, a very high pH value led to the formation of irregular particles. The SEM (Fig. 1) images also show surprisingly high yield (≈100%)

morphologies, i.e., vesicles or WKSS without any other morphology prepared in water or buffer solution (pH 9).

High-resolution transmission electron microscopy images of calcined samples are shown in Figure 2 and Figure S1. Figure 2a shows the presence of aggregated double-layer vesicles with diameters of 50 nm to 150 nm and a wall thickness of 5 nm. Further tuning of the pH of the buffer solution from the value of 5 causes a

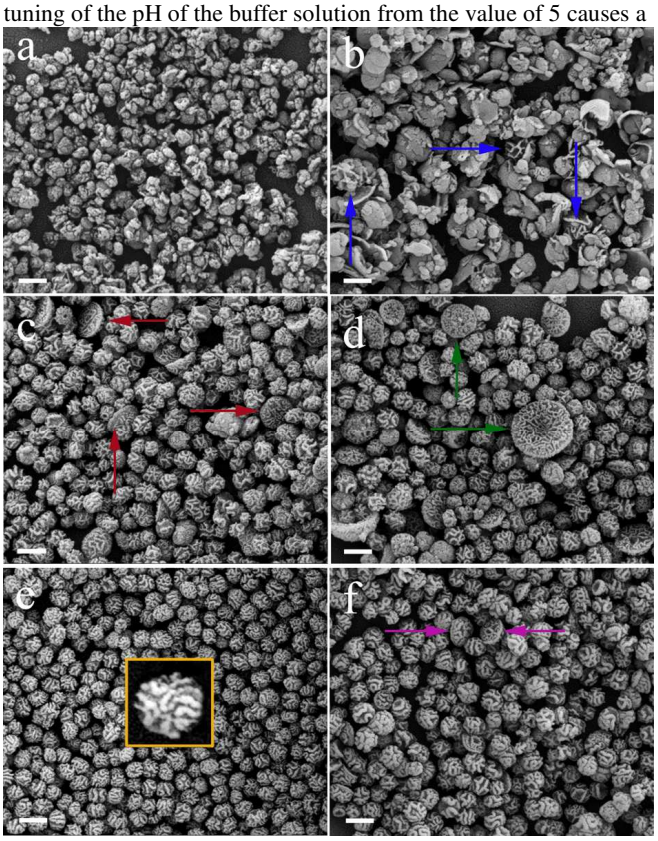

Figure 1. Field emission scanning electron microscopy (FESEM) photographs of (a) VSS, (b) SS5, (c) SS7, (d) SS8, (e) SS9, and (f) SS10. Scale bar = 200 nm. (b) The blue arrow indicates WKSS. (c) The red arrow indicates TSS. (d) The green arrow indicates TSS with different sizes. (e) The inset shows an enlarged image of a WKSS particle. (f) The rose-carmine arrow indicates irregular WKSS.

significant change in the surface features, in addition to the expected breaking of vesicles and aggregation of small particles to form large spheres (Figure 2b), which are induced under acidic conditions (pH = 5);[15] subsequently, walnut-kernel- and tremella-like structures appear to emerge. Increasing pH further to 7, 8, and 10 causes a significant change in the size of the nanoparticles and the pore structure (Figures 2c, 2d, and 2f). As shown in Figures 2c, 2d, and 2f, some U-shaped silica particles conglomerate to form large spherical aggregates, which result in large TSS spheres with a size of approximately 280 nm and a wall thickness ranging from 5 to 15 nm, whereas textural mesopores having sizes ranging from 30 to 40 nm are formed owing to the diameter of the U-shaped silica skeleton or voids between adjacent U-shaped silica particles. Furthermore, all particles exhibit internal mesoporosity with pore diameters ranging from 4 to 5 nm, which is attributed to the removal of the surfactant template.[10] Such hierarchical porosity as an ideal host matrix may be beneficial in applications in many areas such as heterogeneous catalysis, adsorption/separation, and exhaust gas treatment. At a pH of 9.0, uniform WKSS with a size of approximately 100 nm and a wall thickness ranging from 15 to 20 nm was formed (Figure 2f).

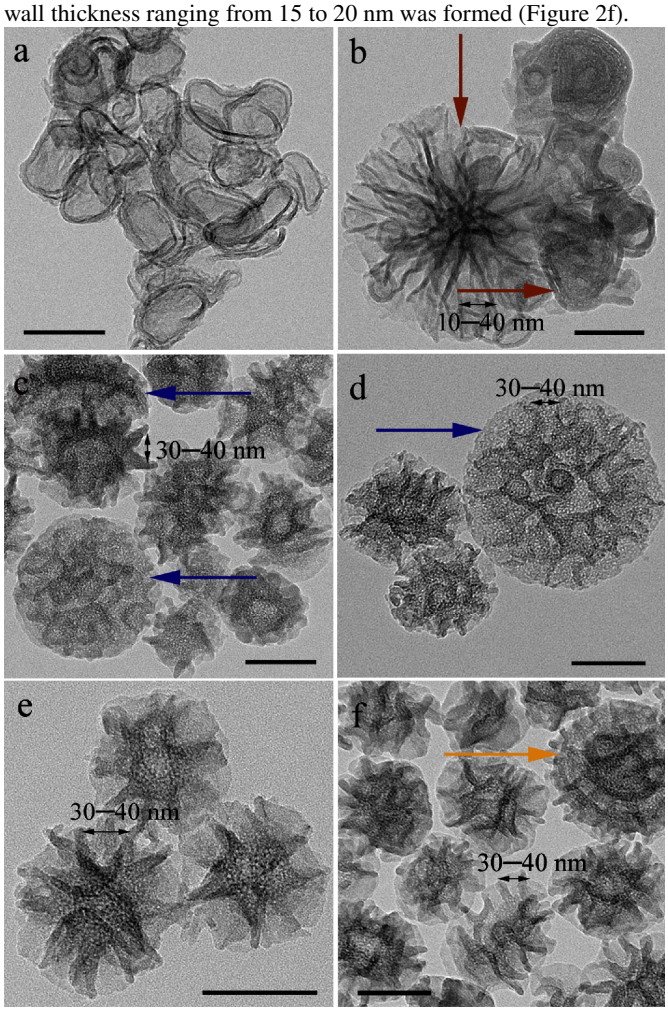

Figure 2. High-resolution transmission electron microscopy (HRTEM) images of (a) VSS, (b) SS5, (c) SS7, (d) SS8, (e) SS9, and (f) SS10. Scale bar = 100 nm. (b) The red arrow indicates VSS and TSS. (c) The blue arrow indicates irregular WKSS and TSS. (d) The blue arrow indicates TSS. (f) The yellow arrow indicates irregular WKSS.

As shown in Figure 3, N_2 sorption analysis was further employed to observe the pore structure of the WKSS and TSS samples. All samples exhibited typical type-IIb isotherms with distinct H3-type hysteresis loops with capillary condensation at P/P_0 ranging from 0.45 to 0.99.[11] The pore size distribution (Figure 3b) centered at approximately 4 nm is attributed to the removal of the surfactants (dual template), and the pore size distribution in the range of 30 to 40 nm may be associated with the diameter of the U-shaped silica skeleton or voids between adjacent U-shaped silica skeletons; these results are in accordance with the TEM results. Additionally, SS-8

exhibits a much larger S_{BET} (252.04 m^2/g) than SS-5 (130.85 m^2/g), SS-7 (78.90 m^2/g), SS-9(94.78 m^2/g), and SS-10 (90.65 m^2/g), as well as a much larger total adsorption pore volume of 0.78 cm^3/g than those of SS-5 (0.60 cm^3/g), SS-7 (0.43 cm^3/g), SS-9 (0.65 cm^3/g), and SS-10 (0. 51 cm^3/g). The ravine structure effectively increased the specific surface area of the walnut-kernel- and tremella-like silica, while the easily accessible high surface areas and active sites inside the pores promote their applications for particular significant mass transport.[18]

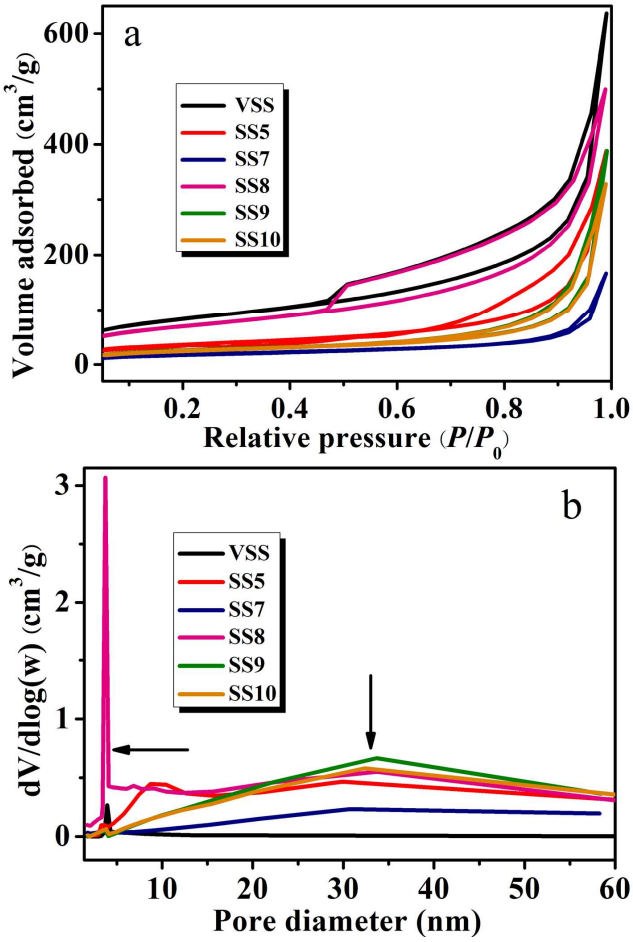

Figure 3. (a) N_2 adsorption–desorption isotherms and (b) corresponding Barrett–Joyner–Halenda (BJH) pore size distribution curves of VSS, SS5, SS7, SS8, SS9, and SS10.

To investigate the sample structure further, small-angle X-ray diffraction experiments were conducted on calcined samples. The results are shown in Figure 4. All samples have one broad peak at approximately 2θ = 1.7°,[12] indicative of a relatively ordered pore structure and relatively stable framework under the reaction conditions.[13]

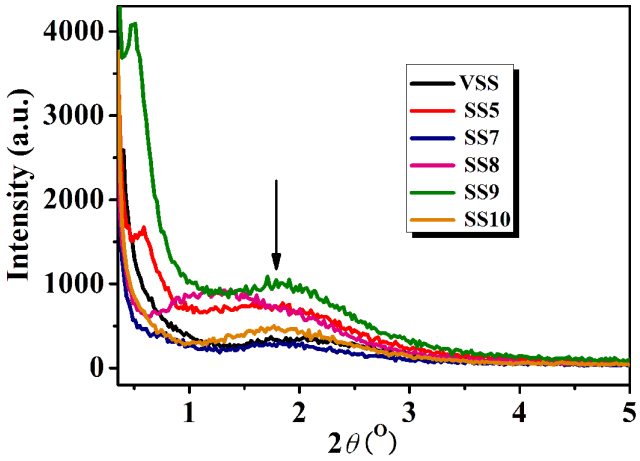

Figure 4. Small-angle X-ray diffraction (SAXRD) patterns of VSS, SS5, SS7, SS8, SS9, and SS10.

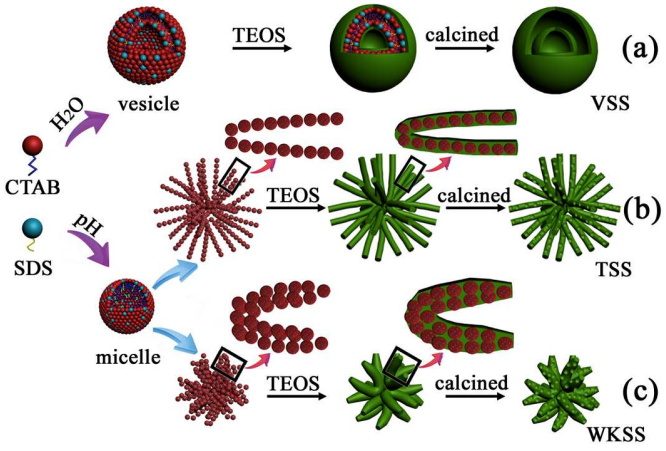

Scheme 1. Schematic representation of proposed formation of (a) VSS, (b) TSS, and (c) WKSS using CTAB and SDS as complex templates.

The proposed structures and the mechanisms for the formation of VSS, WKSS, and TSS in water solutions and buffer solutions with different pH values are illustrated in Scheme 1. In the water solution system (Scheme 1a), both hydrophobic and electrostatic interactions between CTAB and SDS surfactants drove the formation of the stable bilayer vesicle.[14] Careful adjustment of the pH reaction conditions (Scheme 1b and 1c) resulted in the formation of spherical micelles by the CTAB/SDS dual surfactants. Simultaneously, the strong ionic effect from the buffer solution promoted the agglomeration between the spherical micelles, which caused the formation of U-shaped novel micelle aggregates [17]. The U-shaped micelle aggregates further self-assembled into spherical structures with ravined or wrinkled surface through head–head or tail–tail interaction. The diameter of the U-shaped micelle aggregates can vary with a change in the pH value. The U-shaped micelle aggregates slowly interacted because of their similar hydrophilic head groups. The aggregates finally agglomerated into spherical

structures with walnut-kernel- and tremella-like arrangements through self-assembly, in which TEOS can hydrolyze in the hydrophilic units of the aggregates. Then, U-shaped silica particles were formed via the hydrolysis and polycondensation of TEOS. Finally, silica spheres composed of U-shaped mesoporous structures in the U-shaped walls were obtained via calcination to remove the organic template (CTAB/SDS micelle). These particles look like collapsed hollow particles with wrinkled surface.

Conclusions

In summary, WKSS and TSS composed of U-shaped mesoporous structures were fabricated by a pH-induced colloid aggregation method with mixtures of CTAB and SDS used as templates. Because of the rich morphologies of the micelles (e.g., spherical and U-shaped) and the presence of bilayer vesicles, it is anticipated that more novel materials with complex morphologies and hierarchical pore structures can be designed. Furthermore, the particle morphology and its distribution can be adjusted through control of the operation conditions. Morphology transitions of silica nanoparticles prepared in a water solution and in buffer solutions with different pH values occurred in the following order: VSS (H_2O) → TSS and VSS (pH = 5) → WKSS and TSS (pH = 7 and pH = 8) → WKSS (pH = 9) → WKSS and TSS (pH = 10).

Notes and references

[a] Key Laboratory of Fine Chemicals in Universities of Shandong, School of Chemistry and Pharmaceutical Engineering, Qilu University of Technology, Jinan 250353, P. R. China.

[b] College of Chemistry and Chemical Engineering, Xiamen University, Xiamen 361005, P. R. China.

*E-mail: guoweizhou@hotmail.com (G. W. Zhou).

† Electronic Supplementary Information (ESI) available: Characterization of samples. See DOI: 10.1039/c000000x/

1 (a) Y. Chen, H. Chen, J. Shi, *Adv. Mater.*, 2013, **25**, 3144. (b) F. Tang, L. Li, D. Chen, *Adv. Mater.*, 2012, **24**, 1504. (c) Z. Zhou, R. N. K. Taylor, S. Kullmann, H. Bao, M. Hartmann, *Adv. Mater.*, 2011, **23**, 2627. (d) Y. Lu, D. L. Slomberg, B. Sun, M. H. Schoenfisch, *Small*, 2013, **9**, 2189. (e) S. Bégu, R. Durand, D. A. Lerner, C. Charnay, C. Tourné-Péteilh, J. M. Devoisselle, *Chem. Commun.*, 2003, **5,** 640. (f) C. E. Fowler, D. Khushalani, S. Mann, *Chem. Commun.*, 2001, **19**, 2028. (g) Y. Yamauchi, *JCS-Japan*, 2013, **121**, 831. (h) B. G. Trewyn, S. Giri, I. I. Slowing, V, S.-Y. Lin. *Chem. Commun.,* 2007**, 47,** 3236.

2 H. Miyata, K. Kuroda, *Adv. Mater.*, 2001, **13**, 558.

3 (a) A. Chen, M. Komura, K. Kamata, T. Iyoda, *Adv. Mater.*, 2008, **20**, 763. (b) H. Miyata, K. Kuroda, *Adv. Mater.*, 1999, **11**, 857. (c) C. Wang, G. Zhou, Y. Xu, J. Chen, *J. Phys. Chem. C*, 2011, **115**, 22191.

4 D. Zhao, P. Yang, B. F. Chmelka, G. D. Stucky, *Chem. Mater.*, 1999, **11**, 1174.

5 L. M. Bronstein, S. Polarz, B. Smarsly, M. Antonietti, *Adv. Mater.*, 2001, **13**, 1333.

6 S. Guan, S. Inagaki, T. Ohsuna, O. Terasaki, *J. Am. Chem. Soc.*, 2000, **122**, 5660.

7 M. Yu, H. Wang, X. Zhou, P. Yuan, C. Yu, *J. Am. Chem. Soc.*, 2007, **129**, 14576.

8 (a) D. H. W. Hubert, M. Jung, P. M. Frederik, P. H. H. Bomans, J. Meuldijk, A. L. German, *Adv. Mater.*, 2000, **12**, 1286. (b) G. Zhou, Y. Chen, S. Yang, *Microporous Mesoporous Mater.*, 2009, **119**, 223.

9 X. Li, J. He, *ACS Appl. Mater. Interfaces*, 2012, **4**, 2204.

10 J. H. Smått, S. Schunk, M. Lindén, *Chem. Mater.*, 2003, **15**, 2354.

11 G. Leofanti, M. Padovan, G. Tozzola, B. Venturelli, *Catal. Today*, 1998, **41**, 207.

12 P. T. Tanev, Y. Liang, T. J. Pinnavaia, *J. Am. Chem. Soc.*, 1997, **119**, 8616.

13 (a) G. Zhou, Y. Chen, J. Yang, S. Yang, *J. Mater. Chem.*, 2007, **17**, 2839. (b) B. Yang, K. Edler, C. Guo, H. Liu, *Microporous Mesoporous Mater.*, 2010, **131**, 21.

14 J. N. Israelachvili, D. J. Mitchell, B. W. Ninham, *J. Chem. Soc., Faraday Trans. 2*, 1976, **72**, 1525.

15 Y. Zhang, M. H. Yu, L. Zhou, X. F. Zhou, Q. F. Zhao, H. X. Li, C. Z. Yu, *Chem. Mater.* 2008**, 20***,* 6238.

16 T. Sun, Y. M. Li, H. C. Zhang, J.Y. Li, F. F. Xin, L. Kong, A. Y. Hao, *Colloids and Surfaces A: Physicochem. Eng. Aspects,* 2011,**375**, 87.

17 Y. Yan, W. Xiong, X. S. Li, T. Lu, J. B. Huang, Z. C. Li, H. L. Fu, *J. Phys. Chem. B*,2007**,** 111, 2225.

18 V. Polshettiwar, D. Cha, X. X. Zhang, J. M. Basset, *Angew. Chem. Int. Ed.*, 2010, **49**, 9652.